SPECIAL TOPIC
Monitoring China's Environmental Change with Remote Sensing

August 2012 Vol.57 No.22: 2846–2856
doi: 10.1007/s11434-012-5064-8

# Spatial and temporal variations of forest LAI in China during 2000–2010

LIU YiBo[1], JU WeiMin[1*], CHEN JingMing[1], ZHU GaoLong[1,2], XING BaiLing[1], ZHU JingFang[1] & HE MingZhu[1]

[1] *International Institute for Earth System Sciences, Nanjing University, Nanjing 210093, China;*
[2] *Department of Geography, Minjiang University, Fuzhou 350108, China*

Received December 7, 2011; accepted February 6, 2012; published online April 24, 2012

Forests are crucial terrestrial ecosystems. Their leaf area index (LAI) is a key parameter determining the exchange of matter and energy between the atmosphere and the ground surface. In this study, MOD 09A1 and MCD 43A1 data were input into an inversion model based on the 4-scale geometric optical model to retrieve 8-d 500 m LAI products in China during the period 2000 to 2010. The resulting LAI product was validated using LAI measured in 6 typical areas. The spatial and temporal variations of forest LAI and its relationships with temperature and precipitation were analyzed. The results show that the accuracy of the 500 m LAI product was above 70% in the 6 typical areas, indicating the reliability of this product. From 2000 to 2010, forest LAI in northeast, north, and south central China showed increasing trends. However, forest LAI in southeast and parts of southwest China showed downward trends, mainly because of the significant decrease observed during the period 2008 to 2010. Annual mean forest LAI positively correlated with annual mean temperature (AMT) in northeastern China and negatively correlated with AMT in southwest China. It had positive correlations with annual total precipitation in central south and north China. The abnormal climate conditions in 2001 and 2009 caused forest LAI to be obviously lower than normal in regions south of the Qinling Mountains and Huaihe River. Annual mean LAI decreased by more than 1.0 in some areas.

**leaf area index, clumping index, forests of China, MODIS, spatial and temporal variations**

**Citation:** Liu Y B, Ju W M, Chen J M, et al. Spatial and temporal variations of forest LAI in China during 2000–2010. Chin Sci Bull, 2012, 57: 2846–2856, doi: 10.1007/s11434-012-5064-8

Leaf Area Index (LAI) is usually defined as one half of the total green leaf area per unit ground surface area [1]. As an essential parameter characterizing the canopy structure, LAI is highly related to many processes (e.g. photosynthesis, respiration, evapotranspiration, rain interception and energy exchange) [2,3]. It used as an input or state variable for various ecological, biogeochemical, dynamic vegetation, and land surface process models to simulate terrestrial ecosystem-atmosphere interactions at regional and global scales. In recent years, remote sensing techniques rapidly developed and provide new ways to retrieve LAI from large areas [4]. The methods used to retrieve LAI from remote sensing data can be broadly classified into two different groups: statistical models and inverse models [5]. The inversion methods are increasingly being used to generate large regional or global LAI products because of their robust physical basis and nonnecessity of LAI observations. For example, the widely used MODIS LAI product is mainly produced using an inversion method [6,7]. The GLOBCARBON LAI product provided by the European Space Agency is generated using a new LAI retrieval algorithm based on the 4-scale geometrical optical model [8]. This algorithm has been shown to be superior to the MODIS LAI algorithm in studies conducted in Canada, China and other regions [9–11].

LAI directly inversed using remote sensing is effective LAI (LAIe) rather than true LAI (LAI = LAIe/$\Omega$, $\Omega$ is the clumping index, which quantifies the spatial distribution of

*Corresponding author (email: juweimin@nju.edu.cn)

 

canopy leaves [12–14]). However, because of a lack of spatially distributed clumping index data, this parameter is often determined according to land cover types. This approximation induces uncertainties in LAI inversion and model simulations [8,15,16]. Garrigues et al. [17] compared the MODIS, CYCLOPES, GLOBCARBON, and ECOCLIMAP global LAI products and found that their large differences in forest ecosystems were mainly related to whether or not the clumping effects of vegetation canopies were considered.

Compared with LAI inversion from remote sensing, the clumping index retrieval from remote sensing data is less studied. Previous studies mainly focus on clumping index retrieving using Hotspot and Darkspot near-infrared (NIR) reflectance acquired by the multi-angular POLDER sensor [14,18]. However, the spatial resolution (6 km) of clumping index retrieved from POLDER data is too low to meet the demands of generating global 1 km or 500 m LAI products using MODIS data. Recently, Zhu et al. [19] developed a method to retrieve the clumping index over China by simulating the Hotspot and Darkspot reflectance using the MODIS BRDF product, which makes it possible to inverse true LAI using MODIS data at 1 km and 500 m resolutions.

As a crucial terrestrial ecosystem, forests play an important role in climate change and the global carbon cycle [20]. Many studies indicate that forests play a dominant role in the global terrestrial carbon sink [21]. In addition, forest LAI is the key factor influencing carbon sequestration [22], and it directly affects regional or global climate conditions through regulating the partition of sensible and latent heat fluxes [23–25]. Therefore, reliable forest LAI data is a prerequisite to improving the reliability of ecological and land surface process models, and reducing uncertainties in carbon source and sink estimates [26–29].

Affected by the monsoon climate, China’s forests show significant zonality [30]. They include deciduous broadleaf forest (DBF), deciduous needleleaf forest (DNF), evergreen broadleaf forest (EBF), evergreen needleleaf forest (ENF), mixed forest (MF), and shrub (SH) [31,32] (Figure 1). Many studies show that China’s forests are currently acting as a carbon sink [33], which can be attributed to forest expansion and carbon density increases resulting from the implementation of ecological engineering such as conversion of grasslands and croplands to forests, and forest conservation. However, the estimates of the carbon sink of China’s forests derived from different methods are still considerably inconsistent. It is necessary to conduct thorough studies of the spatial and temporal patterns of the carbon cycle in China’s forests and the underlying mechanisms. Therefore, not only are forest LAI products with high quality required, but also the spatial and temporal characteristics of forest LAI need to be analyzed.

In this study, MODIS data were used to derive an LAI inversion model based on the 4-scale geometric optical model to generate 8-d LAI series at a resolution of 500 m for China’s forests during the period 2000 to 2010. The quality of this LAI product was first assessed using field LAI measurements. Then the spatial and temporal variations of LAI and their possible causes were explored to provide a scientific guideline for accurately calculating the carbon budget of China’s forests and comprehensively evaluating the ecological benefits of ecological engineering.

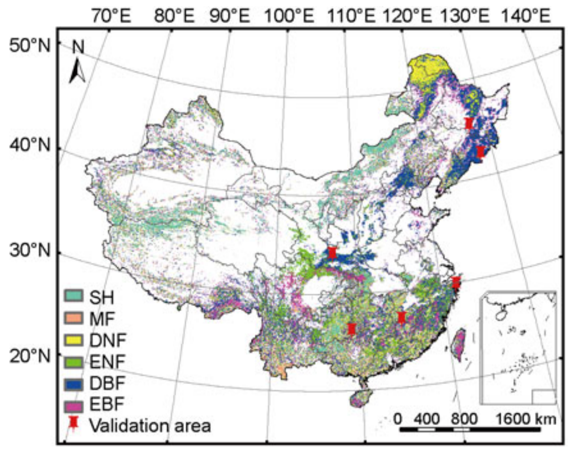


**Figure 1** Spatial distribution of forests in China (based on GLC 2000 land cover data) and areas in which LAI was measured for validating inversed LAI. SH: Shrub; MF: Mixed Forest; DNF: Deciduous Needleleaf Forest; ENF: Evergreen Needleleaf Forest; DBF: Deciduous Broadleaf Forest; EBF: Evergreen Broadleaf Forest.

## 1 Data and methods

### 1.1 Data used

(1) Data for LAI inversion. The data used to retrieve forest LAI in China include the MODIS BRDF product (MCD 43A1) and the corresponding quality product (MCD 43A2), the MODIS surface reflectance product (MOD 09A1), a land cover map (GLC 2000), and digital elevation model (DEM) data (SRTM 4.1, Shuttle Radar Topography Mission) (Table 1). Data format conversion, re-projection, and mosaics were conducted to prepare the input data for the LAI inversion model. The DEM map was used to correct the effect of topography on the retrieved clumping index.

(2) LAI validation data. The quality of the retrieved LAI was evaluated according to the framework “validation of global moderate-resolution LAI products” proposed by CEOS WGCV (“Committee Earth Observing Satellites’ Working Group on Calibration and Validation”) [34]. With the Tracing Radiation and Architecture of Canopy (TRAC) and LAI 2000 instruments, forest LAI and clumping index were measured in 6 representative regions, including Maoershan Mountain in Heilongjiang Province (MES), Changbaishan Mountain in Jilin Province (CBS), Baohe in Shaanxi Province (BH), Tiantong Mountain in Zhejiang Province (TTS), Qianyanzhou in Jiangxi Province (QYZ), and Liping in Guizhou Province (LP) (Table 2).

**Table 1** Data used for retrieving clumping index and LAI

| Data type | Format | Date | Resolution | Sources |
|---|---|---|---|---|
| MCD 43A1 | HDF | 2000-01–2010-12 | 8 d/500 m | Land Processes Distributed Active Archive Center |
| MCD 43A2 | HDF | 2000-01–2010-12 | 8 d/500 m | Land Processes Distributed Active Archive Center |
| MOD 09A1 | HDF | 2000-01–2010-12 | 8 d/500 m | Land Processes Distributed Active Archive Center |
| GLC 2000 | Binary | 2000 | 1 km | European Commission Joint Research Center |
| SRTM 4.1 | ASCII | – | 90 m | International Center for Tropical Agriculture |

**Table 2** The information on 6 sample areas and TM remote sensing data used for validating inversed LAI

| Areas | Geographical ranges | Main forest types | Date | Instruments | Samples | TM/ETM acquired date | Reference |
|---|---|---|---|---|---|---|---|
| MES | 127.50°–127.60°E<br>45.27°–45.33°N | MF | 2009-07 | TRAC<br>LAI2000 | 15 | 2009-06-24 | [35] |
| CBS | 127.81°–128.40°E<br>41.96°–42.58°N | MF | 2002-08 | TRAC | 21 | 2002-08-25 | [37] |
| BH | 106.68°–107.51°E<br>33.65°–34.33°N | DBF | 2003-07 | TRAC | 35 | 2003-06-05 | [38] |
| TTS | 121.70°–121.81°E<br>29.78°–29.86°N | EBF | 2009-09 | TRAC<br>LAI2000 | 21 | 2009-08-18 | [39] |
| QYZ | 114.78°–115.18°E<br>26.54°–26.86°N | ENF | 2008-07 | TRAC | 23 | 2008-07-26 | [36] |
| LP | 108.62°–109.52°E<br>25.73°–26.52°N | EBF | 2003-08<br>2004-08 | TRAC | 19 | 2000-05-14<br>2000-05-21 | [40] |

Landsat Thematic Mapper/Enhanced Thematic Mapper (TM/ETM) data acquired quasi-synchronously with the LAI observation dates were used in conjunction with measured LAI to generate the 30 m TM LAI maps. Then, these TM LAI maps were aggregated to 500 m resolution for evaluating the accuracy of inversed LAI using MODIS data [35,36].

(3) Meteorological data. Daily temperature and precipitation data for the years 2000–2010 observed at national basic meteorological stations were interpolated to generate 500 m temperature and precipitation fields using the inverse distance weighting method. Annual mean temperatures and total precipitation were calculated from the daily data and used to analyze the reasons for the interannual variability of forest LAI. In temperature interpolation, a lapse rate of 6°C per 1000 m was assumed.

### 1.2 LAI inversion based on MODIS data

(1) The MOD 09A1 and GLC 2000 data were input into the LAI inversion model based on the 4-scale geometrical optical model [8] to generate 8-d 500 m LAIe data for 2000–2010. The LAIe data was further smoothed and interpolated using the locally adjusted cubic-spline capping (LACC) method [41].

(2) With the MCD 43A1, MCD 43 A2 data and a modified Ross-Li model [19], the Hotspot (the zenith angles of sun and the sensor were set as 45°, and their relative azimuth angle was 0°) and Darkspot (the zenith angles of sun and the sensor were set as 45°, while their relative azimuth angle was 180°) NIR reflectances were simulated to calculate the Normalized Difference between Hotspot and Darkspot (NDHD). Then the 500 m resolution clumping index was calculated based on its relationship with NDHD. The topography effect on the retrieved clumping index was corrected using the 500 m DEM data [19] and the corrected clumping index was further smoothed using the LACC method [41].

(3) Based on the retrieved clumping index and LAIe data, 8-d LAI maps at 500 m resolution were generated for the period 2000-2010.

### 1.3 Quality assessments of retrieved LAI using the MODIS data

The $R^2$, Root Mean Square Error (RMSE) and Evaluation Accuracy (EA) were used to evaluate the quality of LAI retrieved using the MODIS data. RMSE and EA are calculated as follows:

$$\mathrm{RMSE}=\sqrt{\sum_{i=1}^{N}(\mathrm{LAI_{MOD}}(i)-\mathrm{LAI_{TM}}(i))^2/N}\ , \tag{1}$$

$$\mathrm{EA}=\left[1-\sqrt{\sum_{i=1}^{N}(\mathrm{LAI_{MOD}}(i)-\mathrm{LAI_{TM}}(i))^2/N}\Bigg/\left(\sum_{i=1}^{N}\mathrm{LAI_{TM}}(i)/N\right)\right]\times 100\%, \tag{2}$$

where $\mathrm{LAI_{TM}}(i)$ and $\mathrm{LAI_{MOD}}(i)$ are the resampled TM LAI and inversed LAI values, respectively. $N$ is the number of measured samples used for the validation.

### 1.4 Analysis of the temporal trends of forest LAI

The linear fitting method ($y= ax+b$) was used to analyze the temporal trends of forest LAI:

$$a=\left[n\sum_{i=1}^{n}x_iy_i-\sum_{i=1}^{n}x_i\sum_{i=1}^{n}y_i\right]\Bigg/\left[n\sum_{i=1}^{n}x_i^2-\left(\sum_{i=1}^{n}x_i\right)^2\right], \quad (3)$$

where $n$ is the number of years (equal to 11 in this study), $x_i$ denotes the year (=1, 2, 3, ⋯, 11), $y_i$ represents the annual mean LAI value in the $i$th year. A positive $a$ value means an increased trend in LAI, and *vice versa*.

The interannual variability of LAI was quantified using the Coefficient of Variation (CV):

$$\mathrm{CV}=\sqrt{\sum_{i=1}^{n}(\mathrm{LAI}_i-\overline{\mathrm{LAI}})^2/(n-1)}\Bigg/\overline{\mathrm{LAI}}, \quad (4)$$

where $\mathrm{LAI}_i$ is the annual mean LAI value of the $i$th year, and $\overline{\mathrm{LAI}}$ is the mean LAI during the period 2000–2010.

## 2 Results and analyses

### 2.1 Assessment of the quality of LAI retrieved using the MODIS data

Figure 2 shows the comparison of LAI inversed using MODIS data ($\mathrm{LAI_{MODIS}}$) with measured LAI scaled to 500 m resolution using the TM/ETM data ($\mathrm{LAI_{TM}}$) in 6 typical validation areas. $\mathrm{LAI_{MODIS}}$ agrees well with $\mathrm{LAI_{TM}}$. The scatter points are mostly distributed around the 1∶1 lines, indicating that no systematic biases exist in the retrieved LAI. The $R^2$ of $\mathrm{LAI_{MODIS}}$ ranges from 0.69 (at LP) to 0.80 (at TTS). The $R^2$ values of the other four regions are about 0.75. The RMSE values of $\mathrm{LAI_{MODIS}}$ are in the range 0.50 (at QYZ) to 0.88 (at BH). The EA values of $\mathrm{LAI_{MODIS}}$ are all above 70%, with the highest EA value at CBS (EA=84.9%) and the lowest at LP (EA=70.9%). The relatively poor agreement between $\mathrm{LAI_{MODIS}}$ and $\mathrm{LAI_{TM}}$ at LP was possibly because of the large time lag of LAI measurements compared with the TM image acquisition time and the complex terrain in that area. At MES, the EA value of $\mathrm{LAI_{MODIS}}$ reached 78.6%. However, $\mathrm{LAI_{MODIS}}$ was generally lower than $\mathrm{LAI_{TM}}$. At the plots with high $\mathrm{LAI_{TM}}$ values, the underestimation of $\mathrm{LAI_{MODIS}}$ was more obvious.

In conclusion, forest LAI inversed using the MODIS data is of high quality, and could be used to study the carbon and water cycles of forests in China.

### 2.2 Seasonality of forest LAI in China

Figure 3 shows the maps of inversed forest LAI in January, April, July, and October averaged over the period 2000–2010, which represent the spatial patterns of forest LAI in winter, spring, summer, and autumn, respectively. Inversed forest LAI exhibited distinct spatial and seasonal variations. Summer is the season with the highest LAI, followed by autumn and spring. LAI had the lowest values in winter. Forest LAI shows similar seasonality to temperature, precipitation and incoming solar radiation.

Winter is the season with the lowest temperatures and the least incoming solar radiation. EBF and ENF are still growing slowly in south China, southeast coastal areas, Taiwan,

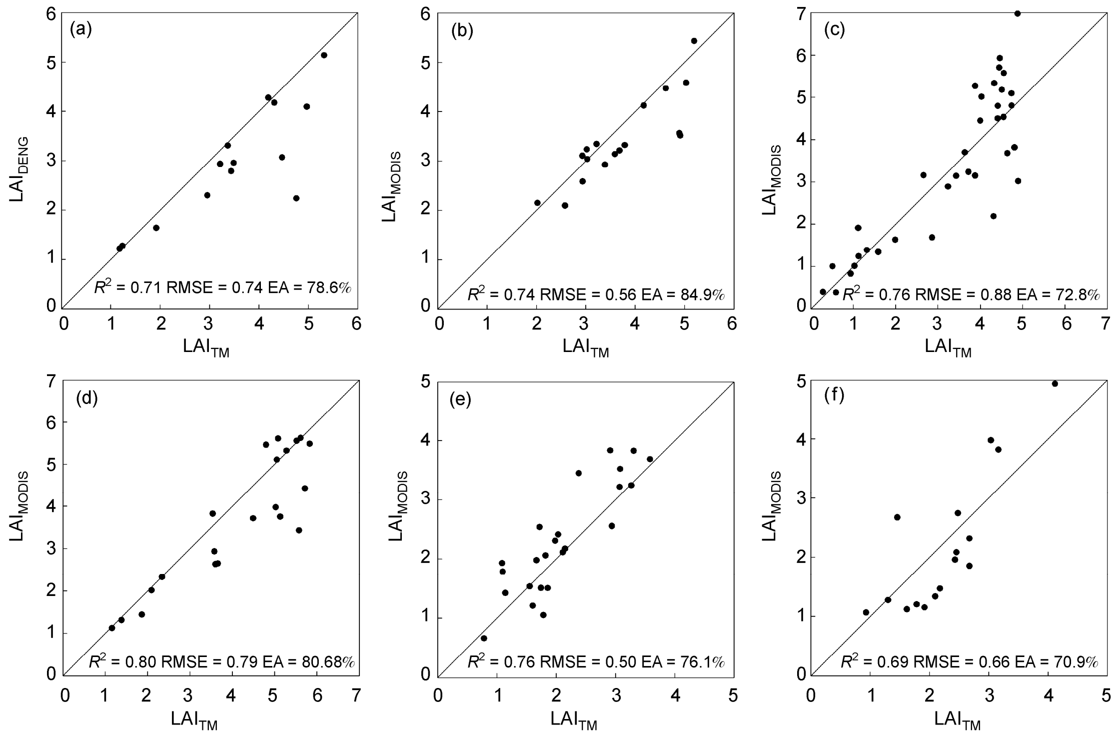


**Figure 2** Validation of inversed LAI in 6 typical forest regions of China. (a) MES; (b) CBS; (c) BH; (d) TTS; (e) QYZ; (f) LP. $\mathrm{LAI_{MODIS}}$ is LAI inversed using MODIS data. $\mathrm{LAI_{TM}}$ is LAI data scaled to 500 m resolution from 30 m LAI maps generated from measured LAI and TM/ETM remote sensing data.

and southwest China. Inversed forest LAI in these regions was greater than 1.0. Forests in most regions of China are in dormancy without growth or leaves. Inversed LAI was generally below 1.0 and approached the annual minimum. As for evergreen forests, inversed LAI in winter might be too low, possibly because of the following two reasons. Firstly, the reflectance spectrum of evergreen leaves is significantly different in winter. The difference in the reflectance of NIR and red bands is relatively smaller in winter than in summer. Secondly, the snowpack accumulated on the ground surface of forests in northern regions might also induce the underestimation of LAI inversed using MODIS data in winter. In spring, temperatures gradually increase from the south to the north, and precipitation simultaneously increases, with forests starting to grow, this is indicated by gradually increasing LAI. The most obvious increase in inversed LAI appeared in the deciduous forests of northeast China and the tropical and subtropical forests south of Qinling. In April, inversed forest LAI was almost above 2.0 in the southeast part of northeast China, and was normally above 3.0 in regions south of Qinling. It was above 4.0 in southeast China as well as Hainan and Taiwan. With the arrival of summer, the summer monsoon gradually moves to the north of the Yangtze River and most regions of north China. Suitable temperatures and abundant rainfall enhance the growth of forests. In summer, inversed LAI approached maximum levels. In July, it was higher than 4.0 in most regions. However, its spatial distribution was significantly affected by water and heat conditions, showing an overall gradual decreasing trend from southeast coastal areas to the northwest areas. Forest LAI in areas north of Da Hinggan Mountains were normally above 8.0. LAI of DBF, DEF, and MF in Xiao Hinggan Mountains and Changbai Mountains, and deciduous forests in north China were in the range 5.0–7.0. In regions dominantly covered by mixed forests such as southeast Tibet and southeast Yunnan province, forest LAI was usually greater than 4.0. As one of the major forest types in China, subtropical EBF is widely distributed in extensive subtropical regions. Their LAI was mostly above 4.0 and even approached 6.0–9.0 in the Hengduan Mountains, Wuyi Mountains and the central Taiwan Province. LAI of most shrubs and open forests in the Xinjiang and Inner Mongolia autonomous regions and Qinghai-Tibet Plateau were below 2.0. In October, forest LAI declined throughout the country. Evergreen forest LAI in south China, southeastern coastal areas, southeast Tibet and Taiwan Province declined slightly. They still ranged from 6.0–8.0. In this season, forests start to drop leaves and stop growth in

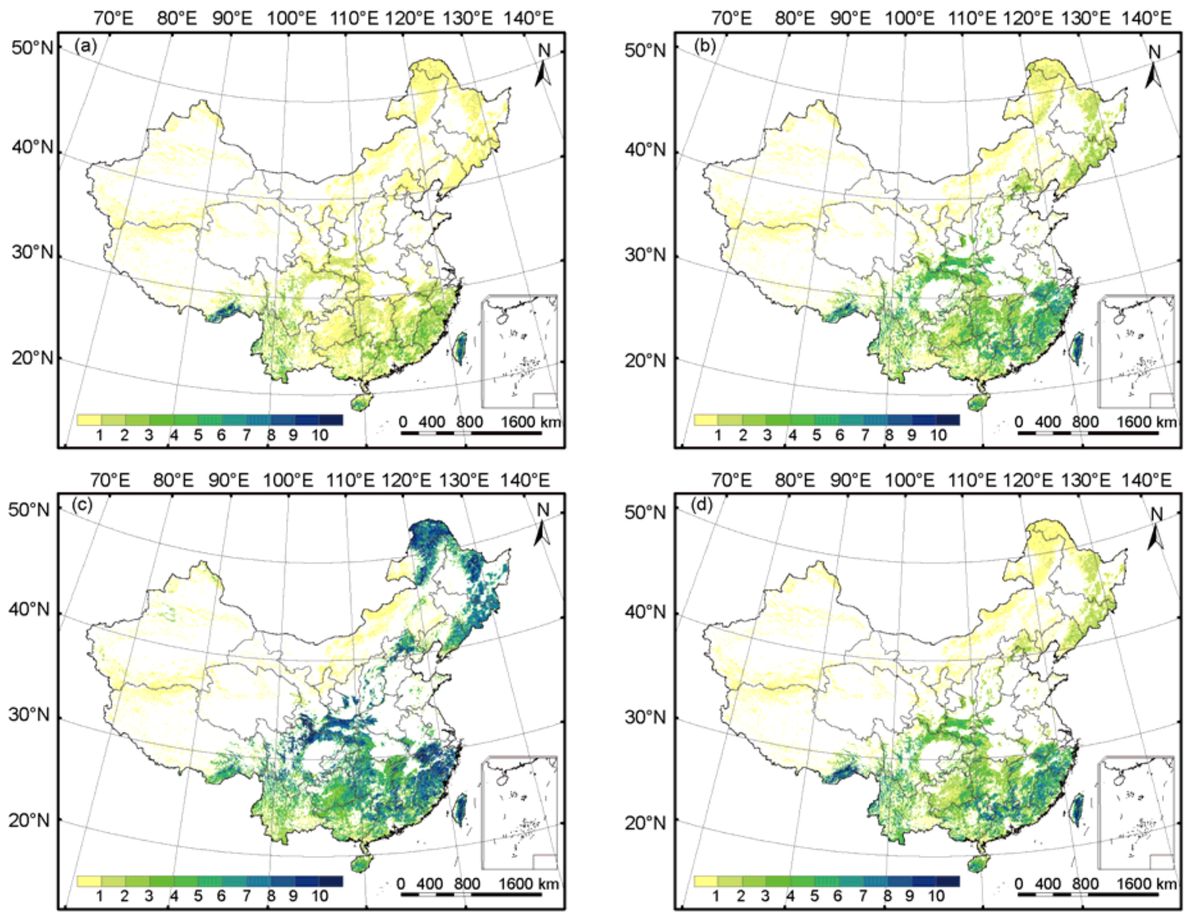


**Figure 3** The spatial patterns of inversed LAI averaged over the period 2000–2010 for forests in China in January (a), April (b), July (c), and October (d).

northeast China because of low temperatures. Inversed LAI here was extensively below 3.0, similar to the values and spatial pattern observed in April. The spatial patterns and seasonal variations of inversed LAI here showed close similarity to the results simulated by the AVIM2 model [42].

### 2.3 Temporal trends of forest LAI in China during the period 2000–2010

Figure 4 shows the temporal trends of annual mean forest LAI in China during the periods 2000–2010 and 2000–2007. There were obvious spatial differences in the temporal trends of forest LAI during the period 2000–2010. Forest LAI increased in northeast, north, northwest, and central China. In Da Hinggan Mountains, Xiao Hinggan Mountains, and eastern Changbai Mountains of northeast China, the northern part of north China, and south Qinling, the annual means of inversed forest LAI increased at rates above 0.03 per year in the 11 years study period. In some areas, the increasing forest LAI rates were even above 0.05 per year. Inversed forest LAI exhibited marginal temporal trends in Inner Mongolia, most of Qinghai-Tibet Plateau, Xinjiang, Yunnan-Guizhou Plateau, and southeast Tibet. The annual means of inversed forest LAI showed obvious downward trends in Zhejiang, Fujian, Guangdong, Jiangxi, and Hunan provinces as well as parts of Sichuan and Yunnan provinces. The decreasing annual mean inversed forest LAI rates were in the range 0.03–0.06. The decreases in annual mean inversed forest LAI in these regions mainly occurred in the years 2008–2010. From 2000 to 2007, the annual mean inversed forest LAI generally increased across the country, at rates above 0.05 per year in most regions (Figure 4(b)).

The national averages of the annual mean inversed LAI of different forest types showed similar annual variations (Figure 5). The inter-annual variability of forest LAI was small during the period 2002–2008. The averages of the annual mean inversed LAI of all forests in China were about 3.0 during this period and dropped to about 2.5 in 2001 and 2009, significantly lower than the normal values.

EBF had the highest annual mean LAI among all types of forests. The national averages of the annual mean LAI of this forest type were around 5.5 in all years with the exceptions of 2001 and 2009. They were less than 5.0 in those two years. As for ENF, the national averages of the annual mean LAI were below 4.0 in 2001 and 2009, also slightly smaller than the values of about 4.5 in other years. The national averages of the annual mean LAI of DBF in 2001 and 2009 were below 3.0, approximately 15% lower than normal values (about 3.5). The national averages of the annual mean LAI of DNF showed obvious periodic oscillations over the 11 years, and obviously decreased in 2001 and 2009 (below 2.5). They were about 2.8 in 2003, 2006, and 2008, slightly lower than the high values of 3.0 in other years. The national averages of the annual mean inversed LAI of MF and SH were relatively small and showed slight inter-annual fluctuations, varying in the ranges 1.5–1.9 and 0.5–0.7, respectively.

The inter-annual variability of annual mean inversed LAI exhibited distinct spatial patterns in China during the period 2000–2010 (Figure 6), indicated by CV values calculated using eq. (4). The CV values of annual mean inversed forest LAI were mostly above 0.06 in northeast, southeast, and central China. They were even above 0.1 in Da Hinggan Mountains region, Jiangxi, Fujian, Hunan, Guizhou and Guangdong, north Sichuan, and south Shaanxi, and between 0.06 and 0.08 in Xiao Hinggan Mountains and Changbai Mountains regions. The inter-annual variability of forest LAI in north China was relatively small, with most CV values in the range 0.04–0.06. The CV values of annual mean inversed LAI ranged 0.04–0.07 in southeast Tibet and west Yunnan-Guizhou Plateau, smaller than the corresponding values in eastern regions at the same latitudes. Inversed forest LAI showed quite small inter-annual variability in Xinjiang, Inner Mongolia, and most parts of Tibet, with CV values generally less than 0.02.

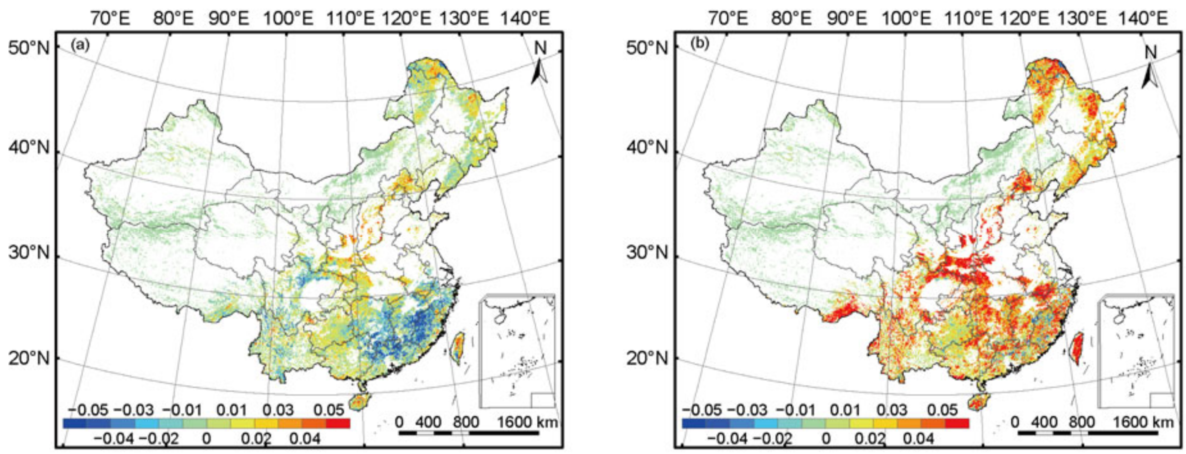


**Figure 4** The temporal trends of annual mean forest LAI in China during the periods 2000–2010 (a) and 2000–2007 (b) ($m^2$ $m^{-2}$ $a^{-1}$).

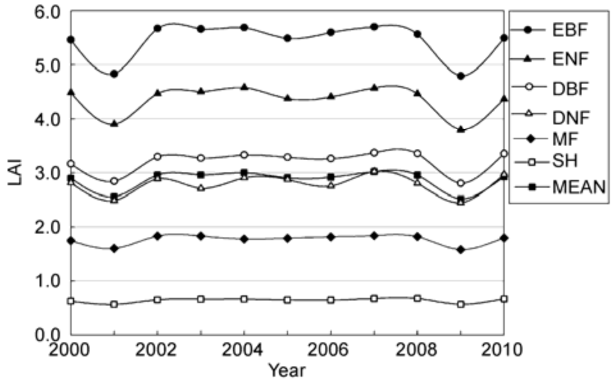


**Figure 5** The national averages of annual mean LAI of different forest types in China over the period 2000–2010.

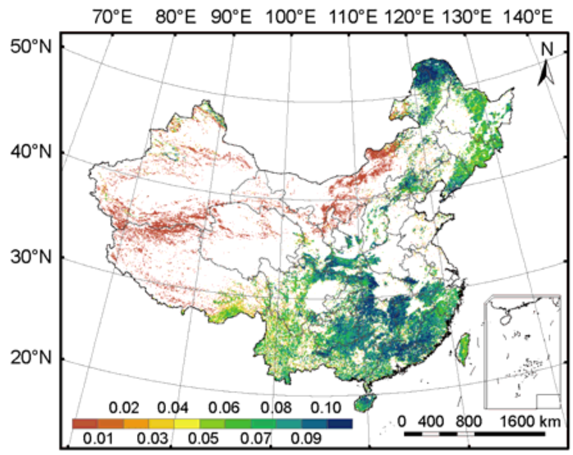

**Figure 6** Distribution of CV values calculated using the annual mean inversed forest LAI in China during the period 2000–2010.

## 2.4 The relationships between forest LAI, temperature and precipitation

Figure 7 shows the relationships between annual mean forest LAI, annual mean temperature and annual total precipitation during the period 2000–2010. In north China, southwest China, southwest Tibet, Yunnan-Guizhou Plateau, south Fujian Province and northeast Guangdong Province, annual mean forest LAI negatively correlated with annual mean temperature, with the correlation coefficients ($r$) between −0.2 and −0.4. In north Yunnan-Guizhou Plateau $r$ values even reached −0.6, significant at a level of 0.05. Annual mean inversed forest LAI was positively correlated with annual mean temperature in northeast China, south Shaanxi Province, Hunan Province, most of Jiangxi Province, north Fujian Province, west Zhejiang Province, and south Anhui Province. The positive correlations between annual mean LAI and annual mean temperature were most significant in northeast China, with $r$ values normally in the range 0.2–0.4 and even above 0.6 in some areas (significant at the 0.05 level). In this region, temperature is one of major factors limiting forest growth [43]. The increase in temperature prolonged the forest growing season and increased annual mean LAI.

Annual mean LAI showed negative correlations with annual total precipitation in the northern part of north China, south China, southeastern coastal areas and west Sichuan Province. The most significant negative correlations appeared in Da Hinggan Mountains and north Xiao Hinggan Mountains regions, with the absolute values of $r$ normally above 0.4. They were even above 0.6 (significant at the 0.05 level) in some areas. In these areas, water is not the major limiting factor for forest growth [44]. Precipitation increases often accompany temperature and incoming solar radiation decreases, which are not favorable for forest growth. In the humid south China and southeast coastal areas, precipitation is abundant and can meet forest growth requirements in normal years. Excessive rainfall often accompanies an increase in clouds and decrease in incoming solar radiation, which limits forest photosynthesis. Annual mean forest LAI and annual total precipitation in these areas also showed negative correlations. Water was a major factor inhibiting the growth of forests in the semiarid northern part of North

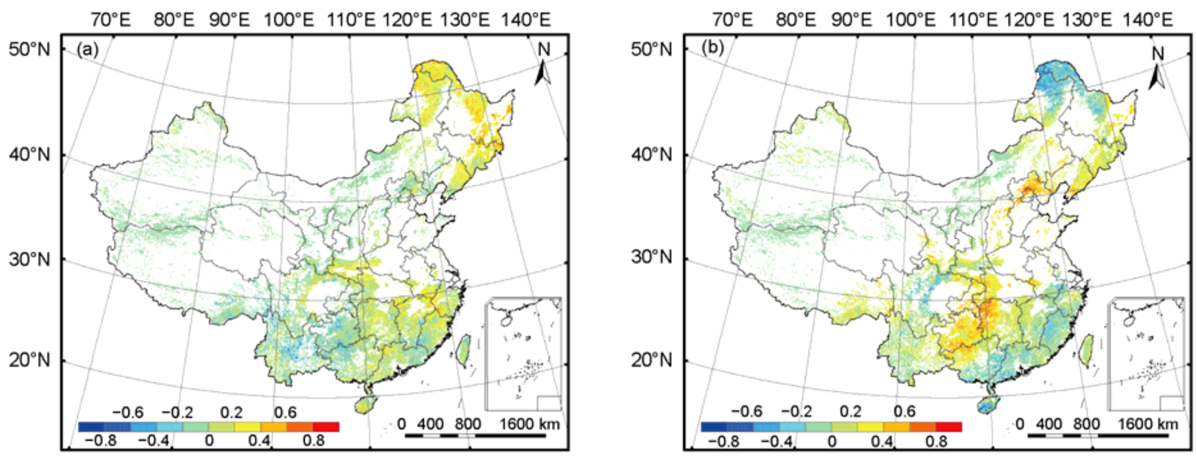


**Figure 7** Spatial distribution of the correlation coefficient of annual mean LAI with temperature (a) and precipitation (b) during the period 2000–2010.

China. Increased precipitation could promote forest growth, and the $r$ values between annual mean forest LAI and annual precipitation were greater than 0.6. Forest LAI was positively correlated with annual total precipitation ($r > 0.4$) in Guizhou Province, west Hunan Province, west Hubei Province, and Chongqing Municipality. Although precipitation in these regions is not too low, poor soil water holding capacity and high evaporation consumption caused by high temperatures make forest growth sensitive to changes in precipitation. Reduced rainfall is detrimental to forest growth and causes forest LAI to decrease.

### 2.5 Analysis of abnormally low LAI of China's forests in 2001 and 2009

In 2001, the annual mean forest LAI was lower than the corresponding values averaged over the period 2000–2010 in most regions of China except for parts of Da Hinggan Mountains, where annual LAI was slightly higher than multi-year means. Compared with the averages during the period 2000–2010, annual mean forest LAI in 2001 was 0.2–0.4 lower in northeast, north and southwest China, 0.6–0.8 lower in the extensive areas south of Qinling and Huaihe (except southwest regions), and even 1.0 lower in southeast coastal regions. Abnormally low LAI in this year was induced by abnormal climate conditions. Precipitation was lower than normal in most regions of China except for Fujian, Guangdong, Guangxi, Yunnan and Sichuan. It was a year of extreme drought following on from 1999 to 2000. Different degrees of drought occurred in all seasons. Annual precipitation was over 360 mm lower than the multi-year averages in the middle reach of the Yangtze River [45]. Especially, droughts occurring during spring and summer in north China, during summer in the middle and lower reaches of the Yangtze River, and during autumn in east China seriously affected terrestrial ecosystems, including forests. In contrast, southwest and south China were hit by severe floods. Annual rainfall in Guangdong and Guangxi was over 360 mm higher than the multi-year averages (Figure 8(c)) [45]. Frosts and cold spells in late spring affected the eastern part of northwest China and north China, Huanghuai Region, and the middle and lower reaches of the Yangtze River [46]. The annual mean temperature in this year was below normal in most regions except parts of southwest China, Inner Mongolia and Xinjiang, where the annual mean temperatures were above normal. The annual mean temperatures were over 0.2°C lower than multi-year averages in Guangxi, Hunan, and Jiangxi provinces and northeast China.

In 2009, the annual mean temperature was 1.0°C lower than multiyear averages in northeast China (Figure 8(e)). Although annual total precipitation was over 70 mm higher than normal, it mainly fell in winter [47]. Low temperatures and snowfall in winter and drought in spring and autumn inhibited forest growth in this region, causing annual mean LAI to decrease by 0.2–0.4. The annual mean temperature of 2009 was relatively high in extensive regions south of Qinling Mountains-Huaihe River. It was 0.2–0.4°C higher than multi-year averages in southern regions of China. The increase of annual mean temperature even reached 0.6°C at the juncture of Sichuan Province and Tibet Autonomous Region (Figure 8(e)). Meanwhile, total annual precipitation was over 150 mm lower than multi-year averages in southern regions of China. The decrease of annual total precipitation was even over 360 mm in Yunnan-Guizhou Plateau and southeast China (Figure 8(f)). The abnormal weather caused forest LAI to decrease more than 0.2 in most regions of China (Figure 8(d)). Compared with multi-year averages from 2000 to 2010, the annual mean forest LAI was over 1.0 lower in southeast Tibet, Sichuan, south Shaanxi, west Hunan, south Anhui, Zhejiang, Fujian, Jiangxi, Hunan, Guangdong, Taiwan, east Guizhou, east Guangxi, and part areas of Yunnan.

## 3 Conclusions

In this study, MODIS data were used to force the LAI inversion model based on the 4-scale geometric optical model to generate 8-d 500 m forest LAI in China during the period 2000–2010. The generated LAI product was validated with LAI measurements scaled up to 500 m resolution using TM/ETM remote sensing data. The spatial and temporal variations of retrieved forest LAI and its relationships with temperature and precipitation were analyzed. Based on this study, the following conclusions can be drawn:

(1) The validations conducted in 6 typical forest regions indicate that the quality of the LAI product generated in this study is reliable. It shows good consistency with LAI produced using LAI field measurements and TM/ETM remote sensing data. The $R^2$ values of this LAI product are above 0.69 and its EA values are above 70% in all 6 regions.

(2) The retrieved LAI of forests in China exhibited distinct seasonality. Summer is the season with highest LAI, followed by spring and autumn. The lowest LAI appeared in winter. The south to north gradient of forest LAI is the smallest in summer. There is a distinct east to west decreasing gradient of forest LAI.

(3) Forest LAI in China showed significant increasing trends during the period 2000–2007. Then it decreased because of the effects of low temperatures in early 2008 in southern regions, and drought and high temperatures in southern regions and low temperatures in northeast regions in 2009. The overall increasing trend of annual mean forest LAI in China was not significant during the period 2000–2010. Annual mean forest LAI even showed significant decreasing trends during this period in Jiangxi, Fujian, east Hunan, and north Guangdong.

(4) The variations in temperature and precipitation induced the inter-annual variability of forest LAI in China.

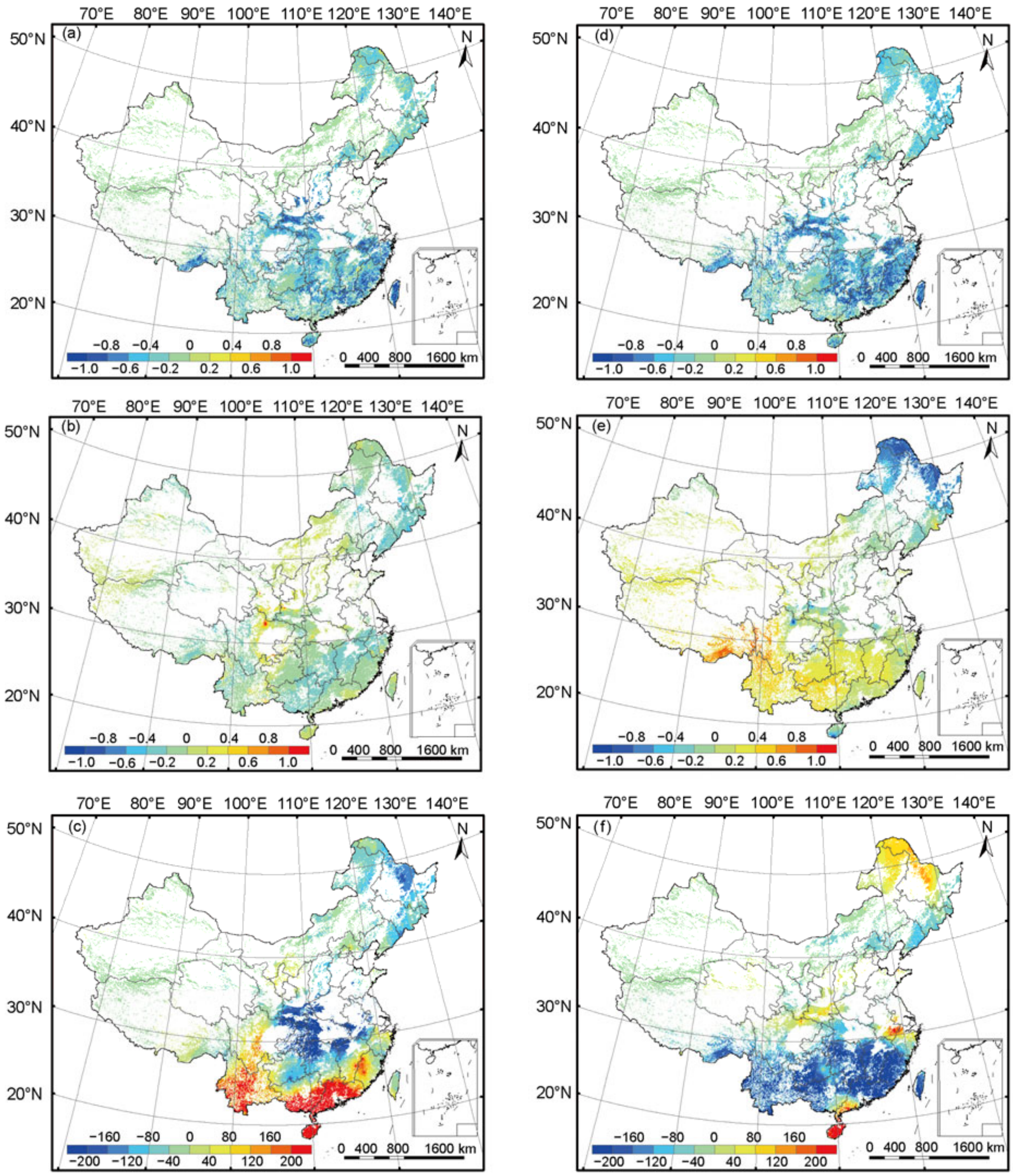


**Figure 8** Spatial distribution of the departures of annual mean LAI ((a), (d)), annual mean temperature (°C) ((b), (e)), and annual total precipitation (mm) ((c), (f)) in 2001(left) and 2009 (right) from multi-year means.

The correlations of annual mean LAI with annual mean temperature and annual precipitation differed spatially. In general, increased temperature may cause forest LAI to increase in northeast China and decrease in southern regions of China. Increased precipitation may cause forest LAI to decrease in north parts of northeast China, southeast China, and south coastal areas of China and to increase in north and central south China.

The quality of the LAI products were individually validated using observations of measured LAI data in 6 typical regions. Forests in China are complex and diverse. Further validation of forest LAI inversed by MODIS data and the model used here should be conducted in more regions. Forest LAI is simultaneously influenced by forest age and environmental factors. For young forests, LAI normally increases with forest age. The relationships between forest LAI, temperature and precipitation were analyzed using the correlation analysis method and showed spatial differences.

These calculated relationships definitely include the effects of forest age on LAI. To identify more realistic forest LAI responses to temperature and precipitation, forest age effects should first be quantified and removed in future studies.

*This work was supported by the National Basic Research Program of China (2010CB833503 and 2010CB0705002), the National High-Technology Research and Development Program of China (2009AA122005) and the Priority Academic Program Development of Jiangsu Higher Education Institutions (PAPD). The authors would like to thank Dr. Fan Wenyi and Dr. Li Mingze of Northeast Forestry University, Tiantong National Station of Forest Ecosystem of East China Normal University, and Qianyanzhou Ecological Station of Chinese Academy of Sciences for help during the field campaigns. We would also like to thank Dr. Zheng Guang (International Institute for Earth System Sciences, Nanjing University), Dr. Sun Rui (Beijing Normal University), and Dr. Chen Xinfang (Hohai University) for providing the leaf area index data of Liping, Changbaishan, and Baohe, respectively.*

1 Chen J M, Black T A. Defining leaf-area index for non-flat leaves. Plant Cell Environ, 1992, 4: 421–429
2 Sprintsin M, Cohen S, Maseyk K, et al. Long term and seasonal courses of leaf area index in a semiarid forest plantation. Agr Forest Meteorol, 2011, 5: 565–574
3 Bonan G B. Forests and climate change: Forcings, feedbacks, and the climate benefits of forests. Science, 2008, 320: 1444–1449
4 Sprintsin M, Karnieli A, Berliner P, et al. The effect of spatial resolution on the accuracy of leaf area index estimation for a forest planted in the desert transition zone. Remote Sens Environ, 2007, 4: 416–428
5 Fang X Q, Zhang W C. The application of remotely sensed data to the estimation of the leaf area index (in Chinese). Reomte Sensing Land Resour, 2003, 3: 58–62
6 Knyazikhin Y, Martonchik J V, Myneni R B, et al. Synergistic algorithm for estimating vegetation canopy leaf area index and fraction of absorbed photosynthetically active radiation from MODIS and MISR data. J Geophys Res-Atmos, 1998, D24: 32257–32275
7 Myneni R B, Hoffman S, Knyazikhin Y, et al. Global products of vegetation leaf area and fraction absorbed PAR from year one of MODIS data. Remote Sens Environ, 2002, 1-2: 214–231
8 Deng F, Chen J M, Plummer S, et al. Algorithm for global leaf area index retrieval using satellite imagery. IEEE Trans Geosci Remote Sensing, 2006, 8: 2219–2229
9 Pisek J, Chen J M, Deng F. Assessment of a global leaf area index product from SPOT-4 VEGETATION data over selected sites in Canada. Can J Remote Sens, 2007, 4: 341–356
10 Liu R, Chen J M, Liu J, et al. Application of a new leaf area index algorithm to China's landmass using MODIS data for carbon cycle research. J Environ Manage, 2007, 3: 649–658
11 Li X F, Ju W M, Zhou Y L, et al. Retrieving leaf area index of forests in red soil hilly region using remote sensing data. In: Zhang X F, Li J, Liu G X, et al., eds. Proceedings-SPIE the International Society for Optical Engineering. USA: International Society for Optical Engineering, 2009. 74710L
12 Nilson T. A theoretical analysis of the frequency of gaps in plant stands. Agr Meteorol, 1971, 8: 25–38
13 Chen J M, Rich P M, Gower S T, et al. Leaf area index of boreal forests: Theory, techniques, and measurements. J Geophys Res-Atmos, 1997, D24: 29429–29443
14 Chen J M, Menges C H, Leblanc S G. Global mapping of foliage clumping index using multi-angular satellite data. Remote Sens Environ, 2005, 4: 447–457
15 Liu J, Chen J M, Cihlar J, et al. Net primary productivity mapped for Canada at 1-km resolution. Glob Ecol Biogeogr, 2002, 2: 115–129
16 Tang S, Chen J M, Zhu Q, et al. LAI inversion algorithm based on directional reflectance kernels. J Environ Manage, 2007, 3: 638–648
17 Garrigues S, Lacaze R, Baret F, et al. Validation and intercomparison of global Leaf Area Index products derived from remote sensing data. J Geophys Res-Biogeosci, 2008, G2: 1–20
18 Lacaze R, Chen J M, Roujean J L, et al. Retrieval of vegetation clumping index using hot spot signatures measured by POLDER instrument. Remote Sens Environ, 2002, 1: 84–95
19 Zhu G L, Ju W M, Chen J M, et al. Foliage clumping index over China's landmass retrieved from the MODIS BRDF products. IEEE Trans Geosci Remote Sensing, 2011, 99: 1–16
20 Yu G R, Zhang L M, Sun X M, et al. Environmental controls over carbon exchange of three forest ecosystems in eastern China. Glob Change Biol, 2008, 11: 2555–2571
21 Pan Y, Birdsey R A, Fang J, et al. A large and persistent carbon sink in the world's forests. Science, 2011, 6045: 988–993
22 Barr A G, Black T A, Hogg E H, et al. Inter-annual variability in the leaf area index of a boreal aspen-hazelnut forest in relation to net ecosystem production. Agr Forest Meteorol, 2004, 13-14: 237–255
23 Hogg E H, Brandt J P, Kochtubajda B. Growth and dieback of Aspen forests in northwestern Alberta, Canada, in relation to climate and insects. Can J Forest Res, 2002, 5: 823–832
24 Margolis H A, Ryan M G. A physiological basis for biosphere-atmosphere interactions in the boreal forest: An overview. Tree Physiol, 1997, 8-9: 491–499
25 Schwartz M D. Phenology and springtime surface-layer change. Mon Weather Rev, 1992, 11: 2570–2578
26 Wang Q, Tenhunen J, Vesala T. Gross primary production simulation in a coniferous forest using a daily gas exchange model with seasonal change of leaf physiological parameters derived from remote sensing data. Int J Remote Sens, 2009, 12: 3013–3025
27 Yuan H, Dai Y J, Xiao Z Q, et al. Reprocessing the MODIS Leaf Area Index products for land surface and climate modelling. Remote Sens Environ, 2011, 5: 1171–1187
28 Luo T X, Neilson R P, Tian H Q, et al. A model for seasonality and distribution of leaf area index of forests and its application to China. J Veg Sci, 2002, 6: 817–830
29 Buermann W, Dong J R, Zeng X B, et al. Evaluation of the utility of satellite-based vegetation leaf area index data for climate simulations. J Clim, 2001, 17: 3536–3650
30 Zhou Y L, Li S Y. China's Forest (in Chinese). Beijing: Science Press, 1990. 20–21
31 Wang S, Chen J M, Ju W M, et al. Carbon sinks and sources in China's forests during 1901-2001. J Environ Manage, 2007, 3: 524–537
32 Fang J Y, Song Y C, Liu H Y, et al. Vegetation-climate relationship and its application in the division of vegetation zone in China. Acta Bot Sin, 2002, 9: 1105–1122
33 Fang J Y, Chen A P, Peng C H, et al. Changes in forest biomass carbon storage in China between 1949 and 1998. Science, 2001, 5525: 2320–2322
34 Morisette J T, Baret F, Privette J L, et al. Validation of global moderate-resolution LAI products: A framework proposed within the CEOS Land Product Validation subgroup. IEEE Trans Geosci Remote Sensing, 2006, 7: 1804–1817
35 Zhu G L, Ju W M, Chen J M, et al. Forest canopy leaf area index in Maoershan Mountain: Ground measurement and remote sensing retrieval (in Chinese). Chin J Appl Ecol, 2010, 8: 2117–2124
36 Li X F, Ju W M, Chen S, et al. Influence of land cover data on regional forest leaf area index inversion (in Chinese). J Remote Sens, 2010, 5: 974–989
37 Wang P, Sun R, Hu J, et al. Measurements and simulation of forest leaf area index and net primary productivity in Northern China. J Environ Manage, 2007, 3: 607–615
38 Chen X F, Chen J M, An S Q, et al. Comparison of different atmospheric correction models in their effects on Landsat TM estimation of forest leaf area index (in Chinese). Chin J Ecol, 2006, 7: 769–773
39 Zhu G L. Retrieval of leaf area index and foliage clumping index from remotely sensed data. Dissertation for the Doctoral Degree. Nanjing: Nanjing University, 2011. 65–67
40 Zheng G, Tian Q J, Chen J M, et al. Combining remote sensing imagery and forest age inventory for biomass mapping (in Chinese). J

Remote Sens, 2006, 6: 932–940
41 Chen J M, Deng F, Chen M Z. Locally adjusted cubic-spline capping for reconstructing seasonal trajectories of a satellite-derived surface parameter. IEEE Trans Geosci Remote Sensing, 2006, 8: 2230–2238
42 Huang M, Ji J J. The spatial-temporal distribution of leaf area index in China: A comparison between ecosystem modeling and remote sensing reversion (in Chinese). Acta Ecol Sin, 2010, 11: 3057–3064
43 Zhu W Q, Pan Y Z, Yang X Q, et al. Study on the effects of climate change on net primary productivity of terrestrial ecosystems in China (in Chinese). Chin Sci Bull (Chin Ver), 2007, 21: 2535–2541
44 Song Y, Ma M G. Variation of AVHRR NDVI and its relationship with climate in Chinese arid and cold region (in Chinese). J Remote Sens, 2008, 3: 499–505
45 Chen Y. Features of weather/climate over China in 2001 (in Chinese). Meteorologica, 2002, 4: 29–33
46 Chen Y. Summary of main meteorological disasters in China in 2001 (in Chinese). J Catastrophol, 2002, 3: 65–70
47 Chen H B, Fan X H. Some extreme events of weather, climate and related phenomena in 2009 (in Chinese). Clim Environ Res, 2010, 3: 322–336